

In Silico tilted properties of the 67–78 fragment of α -synuclein are responsible for membrane destabilization and neurotoxicity

Jean-Marc Crowet,^{1*} Laurence Lins,¹ Ingrid Dupiereux,² Benaïssa Elmoualija,² Aurélien Lorin,¹ Benoit Charlotiaux,¹ Vincent Stroobant,³ Ernst Heinen,² and Robert Brasseur¹

¹Gembloux Agricultural University, Centre de Biophysique Moléculaire Numérique, 2 Passage des Déportés, B-5030 Gembloux, Belgium

²Laboratoire d'Histologie humaine, Centre de Recherche sur les Protéines Prion, Université de Liège, Institut de pharmacie-CHU, 1 Avenue de l'Hôpital, Sart Tilman, B-4000 Liège, Belgium

³Ludwig Institute for Cancer Research - Brussels Branch, 74 Av. Hippocrate, B-1200 Brussels, Belgium

ABSTRACT

α -Synuclein is a 140 residue protein associated with Parkinson's disease. Intraneural inclusions called Lewy bodies and Lewy neurites are mainly composed of α -synuclein aggregated into amyloid fibrils. Other amyloidogenic proteins, such as the β amyloid peptide involved in Alzheimer's disease and the prion protein (PrP) associated with Creutzfeldt-Jakob's disease, are known to possess "tilted peptides". These peptides are short protein fragments that adopt an oblique orientation at a hydrophobic/hydrophilic interface, which enables destabilization of the membranes. In this paper, sequence analysis and molecular modelling predict that the 67–78 fragment of α -synuclein is a tilted peptide. Its destabilizing properties were tested experimentally. The α -synuclein 67–78 peptide is able to induce lipid mixing and leakage of unilamellar liposomes. The neuronal toxicity, studied using human neuroblastoma cells, demonstrated that the α -synuclein 67–78 peptide induces neurotoxicity. A mutant designed by molecular modelling to be amphipathic was shown to be significantly less fusogenic and toxic than the wild type. In conclusion, we have identified a tilted peptide in α -synuclein, which could be involved in the toxicity induced during amyloidogenesis of α -synuclein.

Proteins 2007; 68:936–947.
© 2007 Wiley-Liss, Inc.

Key words: tilted peptides; hydrophobicity; molecular modelling; Parkinson; lipid-interacting peptides.

INTRODUCTION

α -Synuclein (α -syn) is a small protein of 140 residues mainly expressed in neurons in the central nervous system.^{1,2} Intraneural inclusions called Lewy bodies and Lewy neurites are mainly composed of α -syn aggregated into amyloid fibrils and are the common hallmark of several neurodegenerative diseases, including Parkinson's disease and dementia with Lewy bodies.^{3,4} α -Synuclein is unstructured in solution and its helical content increases in the presence of lipids.^{5,6} Structure of the micelle-bound α -syn has been resolved by Ulmer et al.; it forms two anti-parallel curved α -helices (3–37 and 45–92) while the acidic C-terminal tail remains unstructured.⁷ The sequence of α -syn is characterized by seven imperfect repeats of eleven residues in the N-terminal domain, containing two lysines per repeat. This region can form amphipathic α -helices at the liposome surface.⁸ The association between α -syn and the membrane arises from electrostatic and hydrophobic interactions.⁹ Lysines form a charged boundary at the hydrophilic/hydrophobic interface⁸ and it has been shown that α -syn preferentially binds to vesicles containing acidic phospholipids.⁶

The central region of α -syn is crucial for aggregation and cytotoxicity. The region 39–101 forms the fibril core^{10,11} and contains the nonamyloid component, a fragment(61–95) found in amyloid plaques of Alzheimer's disease.^{12,13} Moreover, the peptide 71–82 has been found to be necessary and sufficient for fibril formation.¹⁴ Several fragments of this region are able to aggregate and induce cytotoxicity *in vitro*.^{14–16} El-Agnaf et al.

Abbreviations: α -syn, α -synuclein; A β , β -Amyloid peptide; CHOL, cholesterol; DPX, *p*-xylene-bis-pyridinium bromide; HCA, hydrophobic cluster analysis; HPTS, 8-hydroxypyrene-1,3,6-trisulfonic acid; IMPALA, integral membrane protein and lipid association; LUVs, large unilamellar vesicles; MTS, (3-(4,5-dimethylthiazol-2-yl)-5-(3-carboxymethoxyphenyl)-2-(4-sulfophenyl)-2H-tetrazolium; PC, phosphatidylcholine; PE, phosphatidylethanolamine; PI, phosphatidylinositol; PS, phosphatidylserine; R18, octadecyl rhodamine chloride; SIV, simian immunodeficiency virus; SM, sphingomyelin; SUVs, small unilamellar vesicles.

Grant sponsor: Ministère de la Région Wallonne; Grant numbers: 114915, 215140- α BUSTEC; Grant sponsor: National Fund for Scientific Research of Belgium; Grant number: E.N.R.S.-Televie 7.4.527.05.F; Grant sponsor: Funds for Industrial and Agricultural Research (FRIA).

J.M.C. and L.L. contributed equally to this work.

*Correspondence to: Jean-Marc Crowet, Centre de Biophysique Moléculaire Numérique, FUSAGx, 2 Passage des déportés, B-5030 Gembloux, Belgium. E-mail: crowet.jm@fsagx.ac.be

Received 15 November 2006; Revised 31 January 2007; Accepted 20 February 2007

Published online 6 June 2007 in Wiley InterScience (www.interscience.wiley.com).

DOI: 10.1002/prot.21483

define the peptide 68–76 as the minimum toxic fragment.¹⁶ Moreover, this region shows sequence similarity with domains of the β amyloid peptide (A β) and the PrP protein crucial for aggregation and cytotoxicity.¹⁵

In these two major amyloidogenic proteins implicated in neurodegenerative disorders, we have detected fragments that have an asymmetric distribution of their hydrophobic amino acids when helical, resulting in a hydrophobicity gradient.^{17,18} This property is a feature of the so-called “tilted peptides”.¹⁹ Because of the gradient, tilted peptides adopt an oblique orientation towards a hydrophobic/hydrophilic interface as in biological membranes. This tilted insertion is thought to disturb the parallelism of lipid acyl chains.^{19–21} Indeed, tilted peptides induce liposome fusion, whereas mutations leading to loss of this tilted orientation do not.^{22–24} Furthermore, it should be noted that tilted peptides present a structural lability that could be important for their destabilizing activity.^{24–26} Structural approaches, like polarized infrared spectroscopy (ATR-FTIR), have shown that the fusion depends on the helix formation and orientation into lipid bilayers.^{24,27,28} The existence of this type of peptides has been confirmed by the neutron diffraction studies on the fusion peptide of SIV (Simian immunodeficiency virus)²⁹ and Han et al. have shown by NMR and EPR analysis that the fusion domain of Influenza hemagglutinin HA2 presents an angle close to 40° when inserted into a lipid bilayer.³⁰

Thus tilted peptides often play a functional role in the proteins in which they are found.^{20,31} The presence of such fragments in amyloidogenic proteins has led to the proposal that tilted peptides could be involved in the toxicity associated with them,^{17,18,20} and indeed tilted peptides of A β and PrP were found in areas undergoing conformational changes and known to be important for toxicity.^{17,18,32,33}

Since tilted peptides were detected in A β and PrP, we asked whether such fragments could be present in α -syn. By sequence analysis and molecular modelling, we predicted a tilted peptide corresponding to the 67–78 fragment of α -syn. This peptide was experimentally tested for lipid-mixing and leakage to highlight its lipid destabilizing properties. Its neuronal toxicity was studied using human neuroblastoma cells. Mutants were designed by molecular modelling to assess the role of the hydrophobicity gradient in lipid destabilization and neurotoxicity.

MATERIALS AND METHODS

Materials

Egg phosphatidylcholine (PC), phosphatidylserine (PS), cholesterol (CHOL), and sphingomyelin (SM) were purchased from Sigma (St. Louis, MO). Egg

phosphatidylethanolamine (PE) and phosphatidylinositol (PI) were obtained from Lipid Products (Redhill, Surrey, UK). Octadecyl rhodamine chloride (R18), 8-hydroxypyrene-1,3,6-trisulfonic acid (HPTS), and *p*-xylene-bis-pyridinium bromide (DPX) came from Molecular Probes (Eugene, OR). Buffers used were 10 mM Tris-HCl, 150 mM NaCl, 0.01% EDTA and 1 mM NaN₃ (pH 7.4). Buffers used for circular dichroism measurements were 1 mM Tris-HCl (pH 7.4). All cell culture supplies were purchased from Life Technologies. Peptides were amidated at the C-ter and acetylated at the N-ter. The peptides were synthesized by conventional solid phase peptide synthesis, using Fmoc for transient NH₂-terminal protection and were characterized using mass spectrometry. The α -synuclein peptide (GGAVVTGVTAVA) and the mutant α -synuclein peptide (GGAVSAGVASVT) were 80 and 90% pure, respectively.

Methods

Sequence analysis

The hydrophobic cluster analysis. Hydrophobic cluster analysis (HCA) plot represents the protein sequence as an unrolled cylinder on which the sequence is written to simulate an α -helix. This view is duplicated to restore the environment of each amino acid.³⁴ In this plot, the hydrophobic amino acids (M, I, L, V, F, Y, W) are circled and hatched. Alanine is considered as hydrophobic when it is surrounded by a least three hydrophobic residues. Hydrophobic clusters, varying in length and shape, define specific secondary structures.³⁴

The Jähnig's plot. In the Jähnig's plot, a mean of the hydrophobicity ($\langle H\alpha \rangle$) is attributed to each residue based on a 17-residue window. The Jähnig's equation gives more importance to residues close in terms of secondary structure [see Eq. (1)].³⁵ In this plot, amphipathic α -helix can be predicted as regularly oscillating curve. Tilted peptides are found as ascending or descending oscillations.²⁰

$$\langle H\alpha_{(i)} \rangle = \frac{h_{(i\pm 8)} + h_{(i\pm 7)} + \frac{1}{4}h_{(i\pm 5)} + h_{(i\pm 4)} + \frac{3}{4}h_{(i\pm 3)} + \frac{1}{2}h_{(i\pm 1)} + h_{(i)}}{10} \quad (1)$$

Molecular modelling of the peptides

α -Helical peptides were 3D-built using Hyperchem 6.0 (Hypercube Inc.). As previously described, the α -helix structure is calculated using bond lengths and valence angles of the AMBER united atom forcefield.³⁶ Conformation of the side chains were optimized by the conjugate gradient method of Polak-Ribiere.

The IMPALA method

IMPALA (integral membrane protein and lipid association) is a method that enables simulation of the insertion of a molecule (peptide, protein, drug) into a modelled membrane.³⁷ The latter is described by a function $C_{(z)}$, which varies along the Z axis (outside the membrane, C_z is equal to 1 and in the membrane core, C_z is equal to 0). Hence there is no lipid molecule physically represented. The presence of water (and hence the lipids) is modelled implicitly by the $C_{(z)}$ function that can be considered as the water concentration. Z is normal to the membrane surface and its origin is at the centre of the membrane.

$$C_{(z)} = 1 - \frac{1}{1 + e^{\alpha(|z| - z_0)}} \quad (2)$$

where z_0 and α are fixed at such values that $C_{(-13.5 \text{ \AA})}$ to $C_{(13.5 \text{ \AA})} = 0$, $C_{(18 \text{ \AA})}$ to $C_{(\infty)} = 1$, and $C_{(-18 \text{ \AA})}$ to $C_{(\infty)} = 1$. The $C_{(z)}$ function is continuous and constant in the XY plane. The domain from $|z| = 18$ to 13.5 \AA corresponds to the polar head of lipid and domain from $|z| = 13.5$ to 0 \AA to the hydrophobic tails of phospholipids.³⁷

The interaction between a peptide and the modelled membrane is simulated by the sum of two restraints (E_{env}) that mimic the properties of the membrane: one simulates the hydrophobic effect (E_{int}), which pushes hydrophobic atoms into the membrane, and the other accounts for the lipid-like perturbation (E_{lip}), which is because of the insertion of the molecule in the organized lipid phase.³⁷ For the peptide (or any molecule), each atom contribution is taken into account to provide the total restraint.

$$E_{\text{env}} = E_{\text{int}} + E_{\text{lip}} \quad (3)$$

$$E_{\text{int}} = - \sum_{i=1}^N S_{(i)} E_{\text{tr}(i)} C_{(z_i)} \quad (4)$$

$$E_{\text{lip}} = \alpha_{\text{lip}} \sum_{i=1}^N S_{(i)} (1 - C_{(z_i)}) \quad (5)$$

where N is the total number of atoms, $S_{(i)}$ is the solvent accessible surface of the atom i ; $E_{\text{tr}(i)}$ is the transfer energy of the atom i , and $C_{(z_i)}$ is the value of the $C_{(z)}$ function at the position z_i of the atom i . α_{lip} is a positive empirical factor fixed at 0.018.³⁷

The behavior of peptides in the modelled membrane was analyzed by a systematic procedure. Taking steps of 1 \AA along the Z axis through the membrane, E_{env} was calculated for 5000 random orientations of the peptide in a helical conformation. The position of the structure with the lowest restraint values is considered as the most stable in the bilayer. From there, an IMPALA optimization was performed using a Monte-Carlo simulation of 500 steps. Random rotations of 1° max and random translations of 0.5 \AA max of the peptide were allowed. Side chain motions are taken into account by the angular dy-

namics applied at each step of the IMPALA optimization. Since the lipids are only represented by their properties in IMPALA, it does not permit the effect of the peptide on the lipid structure and hence the membrane disruption to be examined.

Angular dynamics optimization

To analyze structural variations of the peptide inserted in the membrane, we have used the angular dynamics procedure previously defined to simulate the protein folding and described elsewhere.^{38,39}

In the simulations, the total energy (E_{tot}) is the sum of the intramolecular energy of the peptide (E_{intra}) and the energy due to the membrane environment (E_{env}) (see supra). E_{tot} is distributed at each step of the calculation on the peptide torsion k -axis. This total energy is equal to:

$$E_{\text{tot}} = E_{\text{intra}} + E_{\text{env}} = \sum_k E(k) \quad (6)$$

The total energy associated with each torsion axis ($E(k)$) is therefore represented by the sum of the following:

- the torsion energy of the k axis ($E(k)_{\text{tor}}$),
- the intramolecular interaction energies (corresponding to the Van der Waals energy E_{vdw} , the electrostatic energy E_{elec} , and the hydrophobic energy $E_{\text{pho_in}}$) between atoms i and j , divided by the number of axes between these atoms,
- the energy in the membrane for the atoms i and j divided by the number of atoms of the system minus 1 ($N - 1$) and by the number of axes between atoms i and j .

$$E(k) = \underbrace{E(k)_{\text{tor}}}_A + \underbrace{\sum_{i=1}^W \sum_{j=w+1}^N f (E_{\text{vdw}}^{ij} + E_{\text{elec}}^{ij} + E_{\text{pho_in}}^{ij})}_B + \underbrace{\sum_{i=1}^W \sum_{j=w+1}^N f \frac{E_{\text{env}}}{N-1}}_C \quad (7)$$

with $f = 1/\text{number of axes between } i \text{ and } j$.

The energy $E(k)$ enables calculation of an angular dynamics that gives rise to an acceleration of torsion axes. During the dynamics, the length of atomic bonds and the value of valence angles are kept constant, only torsion angles are modified. All calculation of energies, angular acceleration, and rotational velocity are described in details in Lins et al.³⁸

Restraints map

Diagrams showing the restraint values (E_{env}) vs. the angle between the helix axis and the bilayer normal and

vs. the penetration of the center of the mass are obtained as follows: for each degree (angle) and for each Å (penetration), the lowest restraint value obtained during IMPALA simulation is taken. All the points are then joined to generate a 3D-map.

Peptide structure prediction by a stochastic procedure

On the basis of a stochastic algorithm, peptide structures in different environments can be predicted. In the present case, the environment is a lipid bilayer, simulated by IMPALA. The stochastic method uses a de novo search of energy minima by an iterative stochastic procedure and is described in details by Thomas et al.⁴⁰ From the sequence, the procedure generates 100×10^4 structures using ϕ/ψ couples randomly selected among 64 couples derived from the structural alphabet for protein structures proposed by Etchebest et al.⁴¹ At each iteration of 10^4 structures, structure energies are calculated and the values are ranked. Energies calculated for each generated structure include intramolecular energies (Van der Waals, electrostatic, etc.) and IMPALA restraints. The 100 conformations of highest energy on the one hand, and the 100 structures of lowest energy on the other, are compared. When a ϕ/ψ couple yields only energetically unfavorable structures, its probability is decreased for the following iterations. When a ϕ/ψ couple yields only favorable structures, its probability is increased for the following iterations. Calculations are stopped after 100 iterations. Throughout the procedure, structures of low energy are retained; the best 99 models are selected and the energy is minimized using a simplex method.⁴² All energy calculations are described in details elsewhere.⁴⁰ This stochastic algorithm is used by the peptide server PepLook, which was developed by Biosiris-Peptides (Gembloux, Belgium).⁴³

Liposome preparation

Small unilamellar vesicles (SUVs) and large unilamellar vesicles (LUVs) were used in our experiments. These vesicles were prepared from a solution of multilamellar vesicles (MLV) obtained after hydration for 1 h at 37°C of dry lipid films. These films were mixtures by weight of 26.6% PC, 26.6% SM, 26.6% PE, and 20.2% CHOL for neutral liposomes and 30% PC, 30% PE, 2.5% PI, 10% PS, 5% SM, and 22.5% CHOL for acidic liposomes. For the SUV preparation, the MLV suspension was sonicated for 15 min. Following this samples were centrifugated for 10 min at 2000g. LUVs were prepared by the extrusion technique of Mayer et al.⁴⁴ The MLV suspension was submitted to five successive cycles of freezing and thawing and thereafter extruded 10 times through stacked polycarbonate filters (pore size, 0.08 μ M), under a nitrogen pressure of 20 bars using an extruder (Lipex Biomembranes, Vancouver Canada). The concen-

tration of the liposome suspensions was determined by phosphorus analysis.⁴⁵

Lipid-mixing experiments

Mixing of the lipid phase of liposomes can be followed using R18, a lipid soluble probe.⁴⁶ In the labelled liposome population, R18 is self-quenched and represents 6.5% of the total lipid weight. When labelled liposomes fuse to unlabelled liposomes, R18 fluorescence increases due to the probe dilution. The weight ratio of labelled to unlabelled liposomes is 1:4 and the final concentration is between 12.5 and 50 μ M. R18 fluorescence (λ_{exc} , 560 nm; λ_{em} , 590 nm) is measured on a Perkin-Elmer LS-50B fluorimeter.

Leakage of liposome vesicle contents

Membrane perturbation and vesicle release can be measured by the assay of Ellens et al.⁴⁷ based on the quenching of HPTS by DPX. HPTS and DPX were co-encapsulated in the aqueous phase of the same liposomes. When leakage of vesicle content occurs, the quenching by DPX decreases and the fluorescence of HPTS increases. HPTS fluorescence was measured on a Perkin-Elmer LS-50B fluorimeter (λ_{exc} , 360 nm; λ_{em} , 520 nm). Liposomes were prepared as described above but were rehydrated with 1 mL of 12.5 mM HPTS (45 mM NaCl), 45 mM DPX (20 mM NaCl), and 10 mM Tris-HCl at pH 7.4 and passed through a Sephadex G-75 column to removed unencapsulated material.

Circular dichroism measurements

CD spectra were recorded on a Jasco J-815 CD spectrometer with 10-mm path length quartz cuvettes. Ten scans were taken and automatically averaged in the wavelength range from 190 to 250 nm. Peptide secondary structures were determined using CDpro software package, which involved CDSSTR, SELCON3, and CONTINLL methods.⁴⁸ Percentages were calculated by averaging the percentages provided by the three methods. The peptides stock solutions used for the measurements were diluted in 1 mM Tris buffer at pH 7.4, or in TFE to reach a concentration of 10 μ M.

Cell culture

Human SH-SY5Y neuroblastoma cells, kindly provided by Professor Nigel M. Hooper, were cultured in Dulbecco's minimum Eagle medium (DMEM) (Life Technologies) supplemented with 10% fetal bovine serum (FBS) (Life Technologies), 1% penicillin/streptomycin (Life Technologies); cells were maintained at 37°C in a humidified incubator under 95% air and 5% CO₂. For experiments, cells were maintained in FBS-free DMEM medium containing the neuroblastoma growth

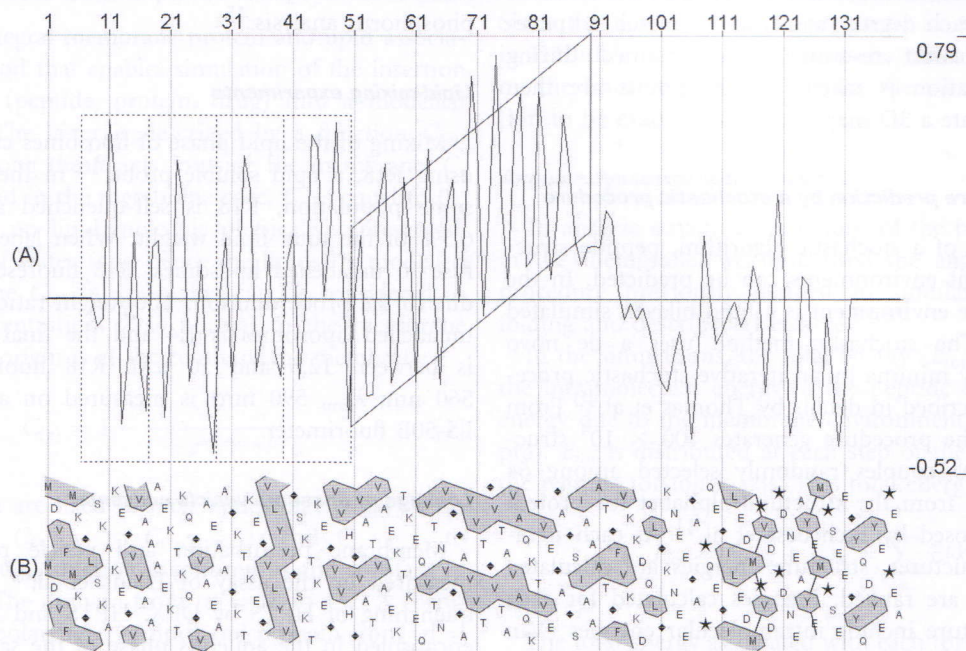


Figure 1

(A) Jähnić profile of the α -synuclein protein. The four first repeats have been boxed (dotted lines) and the domain presenting a hydrophobicity gradient is boxed in continuous line. (B) HCA plot of the α -synuclein sequence. V, F, W, Y, M, L, and I are hydrophobic. These amino acids are circled and hatched to form hydrophobic clusters. G is represented by \blacklozenge and P by a star. By default, A is hydrophilic but when three or more hydrophobic residues surround it, alanine is considered as hydrophobic.

supplement N₂ (Life technologies) and 1% penicillin/streptomycin.

Cell viability assay

Lyophilized 67–78 peptide of α -synuclein and the mutant were dissolved in sterile phosphate-buffered saline at a concentration of 1 mM (stock solution) and freshly prepared aliquots were stored at -20°C until use. For the cellular toxicity experiments, the peptides were dissolved in culture medium to reach the desired concentration (25–400 μM), soon before being added to the cells.

Human SH-SY5Y cells were seeded into 96-well culture plates and allowed to attach. Sixteen hours after seeding, the medium was replaced with serum-free medium containing the neuroblastoma growth supplement N₂ and the cells were treated for 24 h with the indicated concentrations of peptides.

The cell viability was measured using the CellTiter 96 AQueous nonradioactive cell proliferation assay (Promega) according to the manufacturer's instruction. The cell toxicity was assessed quantitatively by MTS assay in the presence of phenazine methosulfate (PMS). After addition of 20 μL of the combined MTS/PMS solution in each well, the plates were incubated at 37°C in a humidified atmosphere containing 5% CO₂ for 2 h. The absorbance

was measured at 490 nm (EL 312e microplate Bio-Tek Instruments).

All MTS assays were performed in triplicate experiments, each repeated three times. MTS assay is a sensitive indicator of mitochondrial activity.

RESULTS

Sequence analysis

Tilted peptides are usually identified using methods based on hydrophobicity such as Jähnić and HCA plots.²⁰ The Jähnić method allocates at each residue a mean hydrophobicity, giving more weight to neighboring residues in terms of secondary structure. In $\langle H\alpha \rangle$ Jähnić profiles, amphipathic helices appear as oscillations with a periodicity of 3–4 amino acids and tilted peptides as increasing or decreasing oscillations, according to the hydrophobic gradient.²⁰ The $\langle H\alpha \rangle$ Jähnić profile of α -syn shows three zones, an amphipathic domain (Sequence 1–50) defined by regular oscillations, a domain presenting increasing hydrophobicity (Sequence 51–89) and a hydrophilic tail (Sequence 90–140) defined by irregular oscillations [Fig. 1(A)]. The first domain corresponds to four imperfect repeats of eleven residues and each presents similar oscillation. However, the 51–89 domain, which

Table I

Mean Hydrophobicity and IMPALA Results for Fragments of the 63–82 Region of α -Synuclein Presenting Tilted Peptide Properties

	Mean hydrophobicity ^a	Mass center position (Å) ^b	Angle of insertion (°) ^c	Peptide sequence
Sequence 63–78	0.56	–8.5	43	VTNVGGAVVTGVTAVA
Sequence 66–78	0.67	–9.3	31	VGGAVVTGVTAVA
Sequence 67–78	0.63	–10	31	GGA VVTGVTAVA
Sequence 68–78	0.65	–10.8	33	GAVVTGVTAVA

^aMean hydrophobicity was calculated using the consensus scale of Eisenberg.⁴⁹

^bThe mass center (MC) position is the distance between the MC and the bilayer center.

^cThe angle is calculated between the helix axis and the bilayer normal.

includes the three other repeats, presents regular ascending oscillations characteristic of tilted peptides. Irregular oscillations of the 90–140 domain indicate that it does not form an amphipathic helix.

HCA plots represent the sequences as α -helices in a 2D view. This graphical representation allows the detection of hydrophobic clusters whose shape and length can be related to secondary structures and hydrophobic properties. The HCA diagram of the α -syn sequence is presented in Figure 1(B). Within the domain presenting increasing hydrophobicity, the 63–82 region is enriched in hydrophobic residues and glycines while containing few polar and charged residues. It was previously shown that tilted peptides present this distribution of amino acids.¹⁹

The two methods suggest that the 63–82 region could contain a tilted peptide. The mean hydrophobicity of tilted peptides, calculated on the basis of the Eisenberg consensus hydrophobicity scale ranges from 0.16 (tilted peptide of lipoprotein lipase) to 0.93 (tilted peptide of SIV).^{31,49} Thus, the mean hydrophobicity of various fragments within the 63–82 region of α -syn was calculated and fragments with a mean hydrophobicity greater than 0.2 were modelled and tested using IMPALA (Table I).

Molecular modelling of the peptides

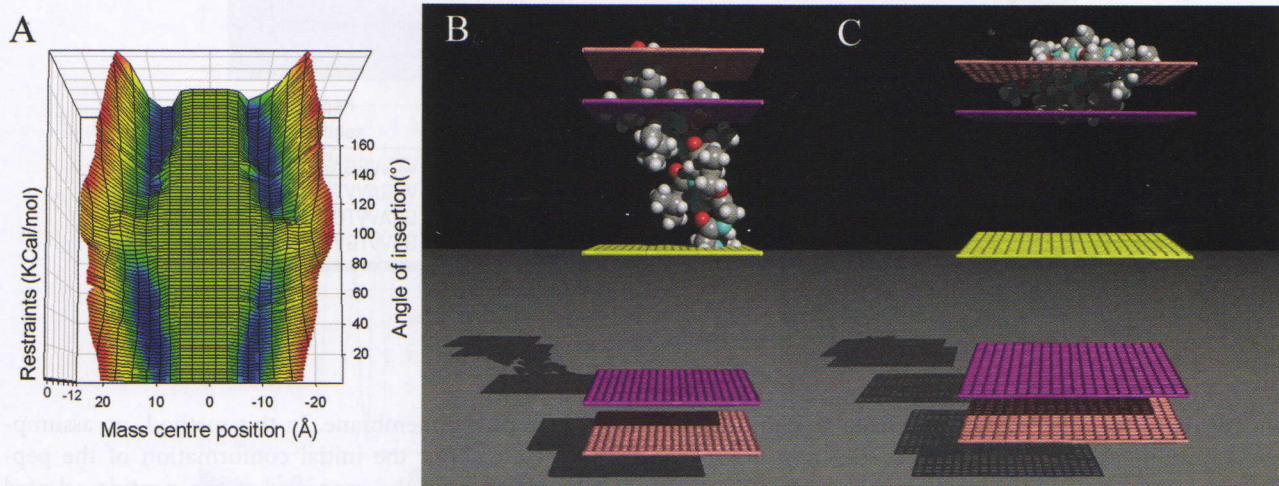
Fragments with sufficient hydrophobicity were then 3D built as helices. To predict their behavior in a membrane, calculations were carried out in three steps. Firstly, an IMPALA systematic procedure was used for the selection of the best tilted peptide from 10 candidates corresponding to different fragments from the 63–82 region. Restraints were calculated for a great number of positions of each peptide in the modelled bilayer. Secondly, an IMPALA optimization was performed from the structure with the lowest restraint value (after the first step) by applying an angular dynamics at each IMPALA step (see methods). This step enables evaluation of the structural fluctuations of the peptide from the alpha helical model. The third step corresponds to the stochastic approach, allowing the analysis of the peptide's structural propen-

sity in the model membrane. In this method, no assumption is made about the initial conformation of the peptide; it starts from the sequence of the peptide selected after the two first steps.

Table I corresponds to the fragments selected after the first calculation step. These fragments present tilted properties, i.e. a high hydrophobicity, a position of the mass center near the phospholipid headgroup/acyl chain interface in the model membrane, and a tilt between 30° and 60°. The 67–78 peptide was chosen for further analysis, since it has a length of 12 residues corresponding to the minimal length for stable helical structure and fits the other criteria of tilted peptides. The most stable position of this fragment corresponds to an angle towards the interface plane around 31° and its mass centre is about 10 Å from the bilayer centre (Table I). Figure 2(A) shows the corresponding restraint map. This peptide is able to adopt four metastable positions within the membrane, two on each side of the membrane. If we consider only a layer, the most stable position corresponds to a tilt between 20° and 40° and a penetration of 10 Å [Fig. 2(A)]. The existence of metastable positions has already been observed for tilted peptides and are thought to contribute to their destabilizing activity.¹⁹

To further predict the structural stability of the helical conformation of the α -syn peptide into a lipid environment and to improve the modelling of the peptide-membrane interaction, angular dynamics were carried out. The peptide remains helical during the procedure (data not shown). The RMS deviation between the structures before and after angular dynamics is 1.48 Å.

To improve the study of the peptide structure in a modelled membrane without allocating an initial secondary structure, an iterative stochastic procedure was used (third step of calculation). After 100 iterations, the results showed that the first three residues of the wild type (WT) peptide adopted a random coil conformation while the other residues were helical. The RMS deviations between the lowest energy structure and the other 98 selected models was under 1 Å, suggesting a low structural lability when the molecule is taken as isolated. Hence, the helical model seems a reasonable hypothesis

**Figure 2**

(A) 3D plot of the 67–78 peptide represents the restraints vs. the helix axis angle (with respect to the bilayer normal) and vs. the mass centre penetration calculated as described in Methods. Restraints increases from blue to red. (B, C) View of the WT peptide and the mutant peptide respectively in the optimal conformation from the stochastic procedure. Mid plane = bilayer center ($z = 0$); first upper (bottom) plane = lipid acid chain/polar headgroups interface at 13.5 Å from the center, second upper (bottom) plane = lipid/water interface ($z = 18$ Å).

for the modelling approach. The stochastic procedure also provides the optimal conformation of peptide in the IMPALA implicit bilayer [Fig. 2(B)].

Design of mutants

To assess the importance of the hydrophobicity gradient for the destabilizing activity of the peptide and hence for the fusion process, “non-tilted” mutants were designed by molecular modelling, as previously shown for other tilted peptides.^{22–24} Mutants were built to adopt a parallel orientation to the lipid bilayer surface. Whenever possible, residue permutations were preferentially chosen; otherwise, substitutions with small amino acids like serine, were carried out.⁵⁰ Sixty five mutants were designed and IMPALA simulations were run for all the peptides. From these simulations, four mutants were predicted to be parallel to the membrane surface. They are listed in Table II. The SynuM53 mutant (2 permutations and 2 substitutions), oriented parallel to the mem-

Table II

Mutants Designed Without Hydrophobicity Gradient

	Mean hydrophobicity ^a	Angle of insertion (°) ^a	Peptide sequence
SynuM40	0.31	86	GGAQVTGVTAAQA
SynuM44	0.47	89	GGAVQAGVATVT
SynuM53	0.52	91.5	GGAVSAGVASVT
SynuM65	0.46	89.5	GGSVTAGVASVT

^aHydrophobicity and angles are calculated as in Table I.

brane, has the mean hydrophobicity value closest to the WT.

The conformation of the mutant was computed by an iterative stochastic procedure, as for the WT [Fig. 2(C)]. The best structures were similar, only the last residue of the mutant adopts a random coil conformation in addition to the three first residues.

Circular dichroism measurements

The secondary structure of the α -syn peptides was evaluated from the measurement of their CD spectra at increasing concentration of TFE. The 67–78 peptide and the SynuM53 mutant undergoes significant structural modifications (from 5 to 40% helix), while increasing the TFE amount (Table III). This suggests a structural plasticity for the peptide, depending on the environment.

Table III

Secondary Structure (%) of the WT and Mutant α -Synuclein Peptides Determined from CD Measurements

	α -Helix (%)	β -Sheet (%)	Turns (%)	Unordered (%)
100% TFE				
WT	40.5	15.5	18.1	26.7
Mutant	39.3	17.9	18.4	24.7
50% TFE				
WT	18.9	22.8	21.9	33
Mutant	17.9	27	21.9	33.1
0% TFE				
WT	5.3	27.1	23.1	42.8
Mutant	5.8	29	22.7	40.2

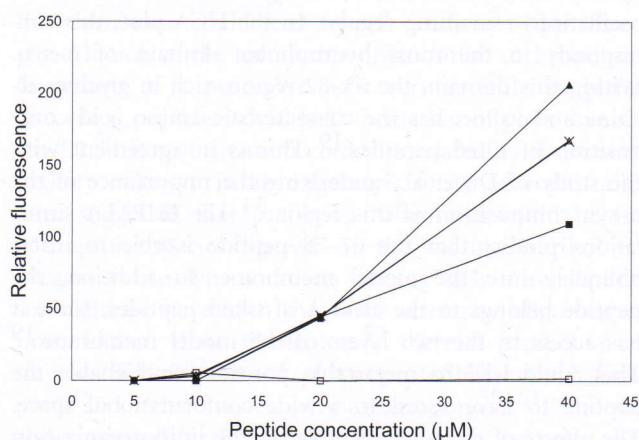


Figure 3

Fusion induced by the α -syn peptide and the synuM53 mutant as a function of peptide concentration. The relative fluorescence of the R18 probe is measured after 15 min of incubation. The fluorescence observed without peptides was subtracted. WT α -syn peptide in the presence of neutral SUVs (\blacktriangle), charged SUVs (\blacksquare), neutral LUVs (\triangle), charged LUVs (\times), and synuM53 mutant in the presence of neutral SUVs (\square).

The structural lability is a feature observed for almost all tilted peptides studied until now.^{24–26} It was shown that increasing the TFE content allows highlighting structural lability.⁵¹

Lipid-mixing and leakage assays

From the modelling approaches, the 67–78 fragment of α -syn was predicted to adopt a tilted orientation to the membranes. Since tilted peptides induce liposome fusion *in vitro* because of their destabilizing activity on membranes,^{17,18,20,22–24} the α -syn tilted peptide was probed for lipid-mixing and leakage experiments.

The peptide, dissolved in TFE or HFP/TFE, was added to a mixture of unlabelled liposomes and R18-labelled liposomes. When lipid-mixing between vesicles occurs, an increase in R18 fluorescence was observed because of the dilution of the lipophilic probe. Different experimental conditions were tested. We have used small (SUV) or large (LUV) liposomes composed of lipids with either a global neutral charge (PC, PE, SM, CHOL) or with acidic lipids (PC, PE, PI, PS, SM, CHOL). The R18 fluorescence intensity was recorded after 15 min. Figure 3 shows that the peptide causes lipid mixing whatever the liposome type (LUV or SUV, with acidic lipids or not) in a concentration-dependent way. This effect was maximal at 40 μ M, corresponding to a molar peptide/lipid ratio of 1.6 (Fig. 3). The mutant peptide was tested in the same conditions as the α -syn WT. The lipid-mixing experiments clearly showed that the synuM53 mutant does not induce significant liposome fusion (Fig. 3). It should be noted that when the peptide solution was

replaced by TFE, no significant effect on R18 fluorescence was observed. This suggests that there was no significant spontaneous vesicle fusion.

To rule out diffusion of R18 without true lipid fusion (due for example to vesicle aggregation) we carried out leakage assays. For this, HPTS and DPX were encapsulated in the same liposomes. When liposomes containing HPTS-DPX are destabilized, the two probes are released into the medium, and there is a dequenching of the HPTS and an increase of fluorescence. Since the lipid-mixing was optimal with uncharged SUVs, only those liposomes were used. Experiments showed that the α -syn tilted peptide induced significant release of HPTS (Fig. 4). Leakage assays also showed almost 50% decrease in HPTS release for the mutant (Fig. 4), confirming a loss of destabilizing capacities, in agreement with the modelling approaches.

In Vitro cytotoxicity of the α -synuclein 67–78 peptide and the SynuM53 mutant on human neuroblastoma cells

Neuronal injuries induced by the α -syn 67–78 peptide were monitored by measuring the reduction of the mitochondrial activity using the MTS assay. MTS is converted to a formazan product by dehydrogenase enzymes, which becomes inactive as the cells suffer. Measurement of this formazan product is an indicator of cell metabolism and viability. As shown on Figure 5, treatment of the α -syn 67–78 peptide induced a concentration-dependent decrease in the number of active cells, while the SynuM53 mutant peptide treatment showed no significant effect. Indeed, MTS reduction (cell viability) was significantly affected by the 67–78 peptide at concentrations from

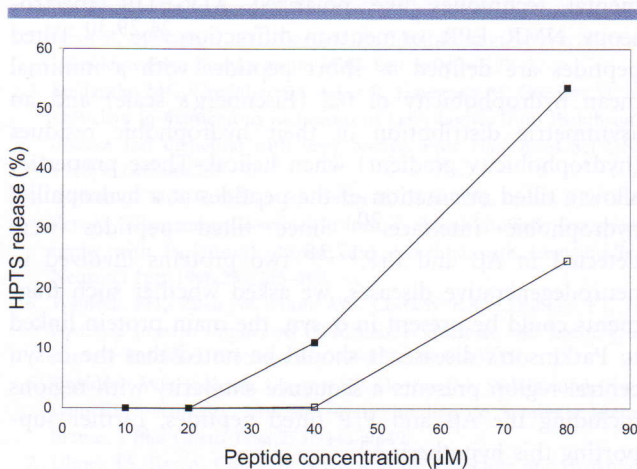


Figure 4

Leakage of neutral SUVs induced by the WT α -syn peptide (\blacksquare) and the synuM53 mutant (\square) as a function of peptide concentration. The relative fluorescence obtained after addition of 25 μ L of Triton X-100 (1%) is 100%. The HPTS fluorescence is measured after 15 min. The fluorescence observed without peptides was subtracted.

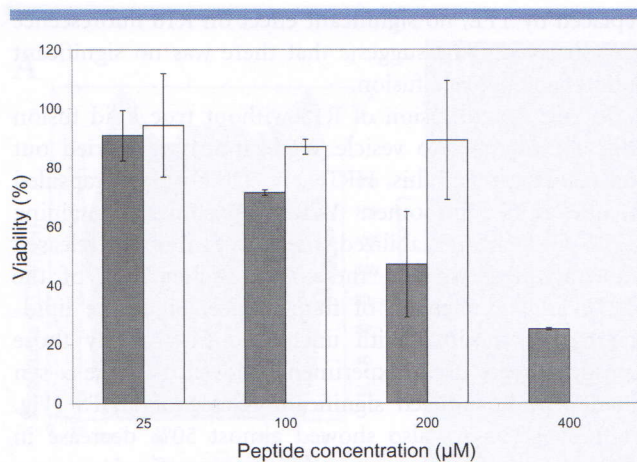


Figure 5

WT α -syn peptide (filled bars) and synuM53 mutant (open bars) were added at concentrations of 25–400M (400M not determined for the synuM53 mutant). Cell metabolism (SH-SY5Y cell line) was measured 24 h later using the MTS assay. Each value represents the mean percentage of cell survival (MTS assay) standard deviations from triplicate experiments repeated three times (nine observations).

400 to 100 μ M over a 24 h period (around 25% viability for 400 μ M). In contrast, the peptide exerted no toxic properties at lower concentrations.

DISCUSSION

The existence of tilted peptides was first predicted by molecular modelling approaches (tilted peptides of NDV (Newcastle disease virus), SIV, BLV (bovine leukemia virus), etc.)^{23,52,53} and supported later by various experimental techniques like polarized ATR-FTIR spectroscopy, NMR, EPR, or neutron diffraction.^{24,29,30} Tilted peptides are defined as short peptides with a minimal mean hydrophobicity of 0.2 (Eisenberg's scale) and an asymmetric distribution of their hydrophobic residues (hydrophobicity gradient) when helical. These properties allow a tilted orientation of the peptides at a hydrophilic/hydrophobic interface.²⁰ Since tilted peptides were detected in A β and PrP,^{17,18} two proteins involved in neurodegenerative diseases, we asked whether such fragments could be present in α -syn, the main protein linked to Parkinson's disease. It should be noted that the α -syn central region presents a sequence similarity with regions including the A β and PrP tilted peptides, further supporting this hypothesis.¹⁵

From the Jähnig's plot, it was predicted that the 1–89 domain of α -syn is amphipathic. This corresponds to the behavior of this protein in presence of lipids.⁶ The structure of the micelle-bound α -syn has been resolved by NMR and it was reported that α -syn forms two anti-parallel amphipathic helices (helix-N 3–37; helix-C 45–92).⁷ On the Jähnig plot, we also observed an increase in

hydrophobicity in the 51–89 region of α -syn, with the oscillations remaining regular. In the HCA plot, this corresponds to the most hydrophobic domain of α -syn. Within this domain, the 63–82 region, rich in glycine, alanine and valine, has the characteristic amino acid composition of tilted peptides.¹⁹ This is in agreement with the study of Du et al., underlying the importance of the α -syn composition of this region.⁵⁴ The IMPALA simulations predict that the 67–78 peptide is able to insert obliquely into the model membrane. In addition, the peptide belongs to the class A of tilted peptides, since it has access to the two layers of the model membrane.¹⁹ This could lead to metastable positions and enable the peptide to have access to a wide conformational space. The effects of the tilted peptide on the lipid organization were further established by studying the molecular interaction between the peptide and the lipid molecules using the Hypermatrix method (data not shown).⁵⁵ The tilted peptide was able to destabilize the lipid organization, inducing a negative monolayer curvature, which was shown to be important in the fusion process.^{19,27}

The dynamic and stochastic calculations showed that when the peptide was taken as an isolated molecule in a hydrophobic environment, the helical conformation appeared very stable. The 99 structures provided by the stochastic procedure were mainly helical. The RMS deviations between structures were under 1 Å.

The 67–78 peptide was further tested *in vitro* for its lipid destabilizing activity. The WT α -syn peptide 67–78 induced fusion and altered the permeability of liposomes and therefore could be considered as belonging to the class of tilted peptides. Fusion was observed with different types of liposome but was more important for the noncharged SUVs. This is in apparent contradiction with the results of Davidson et al., showing that the whole α -syn interacts preferentially with small charged vesicles.⁶ This discrepancy could be due to the fact that the N-terminal domain of α -syn contains positively charged residues that are not present in the 67–78 peptide.

It was previously shown for other tilted peptides, such as the N-terminal domain of the gp32 of SIV, that the hydrophobicity gradient is responsible for the lipid destabilization.²⁴ To test the importance of the hydrophobicity distribution, we designed mutants by molecular modelling, one of which was experimentally probed in detail. Results obtained with the SynuM53 mutant peptide suggest that the lipid destabilization was related to the hydrophobicity gradient. Indeed, the mutant peptide, without a hydrophobicity gradient, did not induce fusion and led to significantly less leakage. The hydrophobic distribution also appeared to have a role in cell toxicity. We showed that the tilted fragment was neurotoxic, inducing the death of neuroblastoma cells, while the nonoblique mutant was not toxic.

How do the tilted properties of the 67–78 α -syn fragment relate to the neurotoxicity of α -syn? Firstly, the

interaction of this fragment in the whole protein with the membrane could lead to cell death by either direct perturbation of the membrane organization or by helping formation of a pore. We have very recently suggested that tilted peptides could help formation of pores in colicin E1.⁵⁶ Pore formation could be related to the neurotoxicity of α -syn in an oligomeric form. Several studies have suggested that prefibrillar oligomers could be the pathogenic species instead of the mature fibrils,^{57,58} because two α -syn mutations causing early-onset Parkinson's disease have been shown to accelerate oligomerization, rather than fibrillation.⁵⁷ Several studies have shown that ring-shaped α -syn protofibrils could form pores and induce vesicle permeabilization.^{59–61} This was also suggested for PrP protein (involved in the prion diseases) and for A β peptide (involved in Alzheimer's disease), where a tilted peptide is also present.^{59,62–64} Though protofibrils are mainly β -structured, they contain some degree of α -helical secondary structure.^{60,65} The α -syn tilted peptide could initiate the destabilization of the membrane under a transient helical conformation, allowing insertion and pore formation, leading to subsequent β structuration into fibrils, in the same way that a helical intermediate is formed during the fibrillogenesis of A β peptide.⁶⁶

On the other hand, a predisposition to amyloid formation could also be related to the position of the 67–78 fragment in α -syn: It lies in a region that undergoes transconformation. Indeed, the central region of α -syn appears to be very important for transconformation and neurotoxicity, being notably found in the core region of amyloid fibrils.^{10,11} Truncation of the C-terminal domain of α -syn induces faster aggregation than the full-length molecule.⁶⁷ Giasson et al. have previously suggested that a peptide of 12 amino acids (residues 71–82) from the hydrophobic domain of α -syn is necessary and sufficient for fibrillation. Introduction of a charged residue in this peptide decreased the polymerization rate, and a deletion prevented the polymer formation.¹⁴ In contrast, El-Agnaf et al. have determined from a systematic research of aggregation properties and toxicity of α -syn fragments that the 68–78 peptide is the shortest fragment retaining aggregation properties and toxicity.¹⁶ It is important to note that tilted peptides are structurally labile.^{24–26} The α -syn protein shows this increase in lability, by being random in solution, and the N-terminal domain of α -syn is helical in the presence of lipids and depending on the conditions, it forms amyloid fibrils, which are β structured.^{5,7,11} This is detected in CD experiments that show that increasing the TFE content increases the helical conformation of the 67–78 fragment, from 5 to 40%. We suggest that amyloidogenic proteins could need structurally labile regions to initiate the whole transconformation. Thus, initiation of the transconformation could be assumed by tilted peptides. This has also been proposed for PrP and A β peptide.^{18,20}

In the future, this work could contribute to a new pharmacological approach for neurotoxic diseases. Tilted peptides have the potential to provide a target for molecules, which could decrease or abolish their destabilizing activities. This was notably shown for the A β tilted peptide whose fusogenic capacities are significantly decreased by specific hydrophobic interactions with amphipathic apolipoprotein E helices.^{68,69} Derivatives of those helices were designed by molecular modelling and shown to be more efficient in terms of inhibitory effects.⁷⁰

In conclusion, we have shown that the 67–78 peptide of α -syn is able to induce liposome destabilization and neurotoxicity, as predicted by molecular modelling approaches. Though the tilted insertion has not been firmly proved experimentally, we assume that the α -syn peptide presents all the properties of the “tilted peptide family” since introducing a mutation that alters the tilted peptide structure clearly showed that there was a correlation between the lipid insertion and the destabilizing activity of the peptide, on liposomes as well as on cells. These tilted properties could be involved in the neurotoxicity of α -syn, either by direct perturbation of cell membrane or by helping formation of a pore.

ACKNOWLEDGMENTS

L.L. and R.B. thank the National Funds for Scientific Research (FNRS) of Belgium, where they are Research Associate and Research Director, respectively. We are grateful to Dr. P. Talmud for reading the manuscript.

REFERENCES

1. Maroteaux L, Campanelli JT, Scheller RH. Synuclein: a neuron-specific protein localized to the nucleus and presynaptic nerve terminal. *J Neurosci* 1988;8:2804–2815.
2. Jakes R, Spillantini MG, Goedert M. Identification of two distinct synucleins from human brain. *FEBS Lett* 1994;345:27–32.
3. Spillantini MG, Crowther RA, Jakes R, Hasegawa M, Goedert M. α -Synuclein in filamentous inclusions of Lewy bodies from Parkinson's disease and dementia with lewy bodies. *Proc Natl Acad Sci USA* 1998;95:6469–6473.
4. Spillantini MG, Crowther RA, Jakes R, Cairns NJ, Lantos PL, Goedert M. Filamentous α -synuclein inclusions link multiple system atrophy with Parkinson's disease and dementia with Lewy bodies. *Neurosci Lett* 1998;251:205–208.
5. Weinreb PH, Zhen W, Poon AW, Conway KA, Lansbury PT, Jr. NACP, a protein implicated in Alzheimer's disease and learning, is natively unfolded. *Biochemistry* 1996;35:13709–13715.
6. Davidson WS, Jonas A, Clayton DF, George JM. Stabilization of α -synuclein secondary structure upon binding to synthetic membranes. *J Biol Chem* 1998;273:9443–9449.
7. Ulmer TS, Bax A, Cole NB, Nussbaum RL. Structure and dynamics of micelle-bound human α -synuclein. *J Biol Chem* 2005;280:9595–9603.
8. Bussell R, Eliezer D. A structural and functional role for 11-mer repeats in α -synuclein and other exchangeable lipid binding proteins. *J Mol Biol* 2003;329:763–778.
9. Zhu M, Li J, Fink AL. The association of α -synuclein with membranes affects bilayer structure, stability, and fibril formation. *J Biol Chem* 2003;278:40186–40197.

10. Miatek H, Mizusawa H, Iwatsubo T, Hasegawa M. Biochemical characterization of the core structure of α -synuclein filaments. *J Biol Chem* 2002;277:19213–19219.
11. Del Mar C, Geenbaum EA, Mayne L, Englander SW, Woods V. Structure and properties of α -synuclein and other amyloids determined at the amino acid level. *Proc Natl Acad Sci USA* 2005;102:15477–15482.
12. Ueda K, Fukushima H, Masliah E, Xia Y, Iwai A, Yoshimoto M, Otero DA, Kondo J, Ihara Y, Saitoh T. Molecular cloning of cDNA encoding an unrecognized component of amyloid in Alzheimer disease. *Proc Natl Acad Sci USA* 1993;90:11282–11286.
13. Iwai A. Properties of NACP/ α -synuclein and its role in Alzheimer's disease. *Biochim Biophys Acta* 2000;1502:95–109.
14. Giasson BI, Murray IV, Trojanowski JQ, Lee VM. A hydrophobic stretch of 12 amino acid residues in the middle of α -synuclein is essential for filament assembly. *J Biol Chem* 2001;276:2380–2386.
15. El-Agnaf OMA, Bodles A, Guthrie DJS, Harriott P, Irvine GB. The N-terminal region of non-A β component of Alzheimer's Disease amyloid is responsible for its tendency to assume β -sheet and aggregate to form fibrils. *Eur J Biochem* 1998;258:157–163.
16. El-Agnaf OMA, Irvine GB. Aggregation and neurotoxicity of α -synuclein and related peptides. *Biochem Soc Trans* 2002;30:559–565.
17. Pillot T, Goethals M, Vanloo B, Talussot C, Brasseur R, Vandekerckhove J, Rosseneu M, Lins L. Fusogenic properties of the C-terminal domain of the Alzheimer β -amyloid peptide. *J Biol Chem* 1996;271:28757–28765.
18. Pillot T, Lins L, Goethals M, Vanloo B, Baert J, Vandekerckhove J, Rosseneu M, Brasseur R. The 118–135 peptide of the human prion protein forms amyloid fibrils and induces liposome fusion. *J Mol Biol* 1997;274:381–393.
19. Lins L, Charlotiaux B, Thomas A, Brasseur R. Computational study of lipid-destabilizing protein fragments: towards a comprehensive view of tilted peptides. *Proteins* 2001;44:435–447.
20. Brasseur R. Tilted peptides: a motif for membrane destabilization (Hypothesis). *Mol Membr Biol* 2000;17:31–40.
21. Colotto A, Martin I, Ruyschaert JM, Sen A, Hui SW, Epand RM. Structural study of the interaction between the SIV fusion peptide and model membranes. *Biochemistry* 1996;35:980–989.
22. Pérez-Méndez O, Vanloo B, Decout A, Goethals M, Peelman F, Vandekerckhove J, Brasseur R, Rosseneu M. Contribution of the hydrophobicity gradient of an amphipathic peptide to its mode of association with lipids. *Eur J Biochem* 1998;256:570–579.
23. Horth M, Lambrecht B, Khim MCL, Bex F, Thiriart C, Ruyschaert JM, Burny A, Brasseur R. Theoretical and functional analysis of the SIV fusion peptide. *EMBO J* 1991;10:2747–2755.
24. Martin I, Dubois MC, Defrise-Quertain F, Saermark T, Burny A, Brasseur R, Ruyschaert JM. Correlation between fusogenicity of synthetic modified peptides corresponding to the NH₂-terminal extremity of simian immunodeficiency virus gp32 and their mode of insertion into the lipid bilayer: an infrared spectroscopy study. *J Virol* 1994;68:1139–1148.
25. Charlotiaux B, Lorin A, Crowet JM, Stroobant V, Lins L, Thomas A, Brasseur R. The N-terminal 12 residue long peptide of HIV gp41 is the minimal peptide sufficient to induce significant T-cell-like membrane destabilization in vitro. *J Mol Biol* 2006;359:597–609.
26. Lorin A, Thomas A, Stroobant V, Brasseur R, Lins L. Lipid-destabilising properties of a peptide with structural plasticity. *Chem Phys Lipids* 2006;141:185–196.
27. Martin I, Schaal H, Scheid A, Ruyschaert JM. Lipid membrane fusion induced by the human immunodeficiency virus type 1 gp41 N-terminal extremity is determined by its orientation in the lipid bilayer. *J Virol* 1996;70:298–304.
28. Castano S, Desbat B. Structure and orientation study of fusion peptide FP23 of gp41 from HIV-1 alone or inserted into various lipid membrane models (mono-, bi- and multibi-layers) by FT-IR spectroscopies and Brewster angle microscopy. *Biochim Biophys Acta* 2005;1715:81–95.
29. Bradshaw JP, Darkes MJ, Harroun TA, Katsaras J, Epand RM. Oblique membrane insertion of viral fusion peptide probed by neutron diffraction. *Biochemistry* 2000;39:6581–6585.
30. Han X, Bushweller JH, Cafiso DS, Tamm LK. Membrane structure and fusion-triggering conformational change of the fusion domain from influenza hemagglutinin. *Nat Struct Biol* 2001;8:715–720.
31. Brasseur R, Pillot T, Lins L, Vandekerckhove J, Rosseneu M. Peptides in membranes: tipping the balance of membrane stability. *Trends Biochem Sci* 1997;22:167–171.
32. Lansbury PTJ, Costa JM, Griffiths EJ, Simon EJ, Auger M, Halverson KJ, Kocisko DA, Hendsch ZS, Ashburn TT, Spencer RG. Structural model for the β -amyloid fibril based on interstrand alignment of an antiparallel-sheet comprising a C-terminal peptide. *Nat Struct Biol* 1995;2:990–998.
33. Nguyen J, Baldwin MA, Cohen FE, Prusiner SB. Prion protein peptides induce α -helix to β -sheet conformational transitions. *Biochemistry* 1995;34:4186–4192.
34. Gaboriaud C, Bissery V, Benchetrit T, Mornon JP. Hydrophobic cluster analysis an efficient new way to compare and analyse amino acid sequence. *FEBS Lett* 1987;224:149–155.
35. Jahnig F. Structure predictions of membrane proteins are not that bad. *Trends Biochem Sci* 1990;15:93–95.
36. Brasseur R, Lins L, Vanloo B, Ruyschaert JM, Rosseneu M. Molecular modelling of the amphipathic helices of the plasma apolipoproteins. *Proteins* 1992;13:246–257.
37. Ducarme P, Rahman M, Brasseur R. Impala: a simple restraint field to simulate the biological membrane in molecular structure studies. *Proteins* 1998;30:357–371.
38. Lins L, Charlotiaux B, Heinen C, Thomas A, Brasseur R. "De novo" design of peptides with specific lipid-binding properties. *Bioophys J* 2006;90:470–479.
39. Brasseur R. Simulating the folding of small proteins by use of the local minimum energy and the free solvation energy yields native-like structures. *J Mol Graph* 1995;13:312–322.
40. Thomas A, Deshayes S, Decaffmeyer M, Van Eyck MH, Charlotiaux B, Brasseur R. Prediction of peptide structure: How far are we? *Proteins* 2006;65:889–897.
41. Etchebest C, Benros C, Hazout S, de Brevern AG. A structural alphabet for local protein structure: improved prediction methods. *Proteins* 2005;59:810–827.
42. Nelder JA, Mead RA. A simplex method for function minimization. *Comput J* 1997;7:303–313.
43. http://www.biosiris.com/en/Online_order/PepLook/PepLook_order.html.
44. Mayer LD, Hope MJ, Cullis PR. Vesicles of variable sizes produced by a rapid extrusion procedure. *Biochim Biophys Acta* 1986;858:161–168.
45. Mrsny RJ, Volwerk JJ, Griffith OH. A simplified procedure for lipid phosphorus analysis shows that digestion rates vary with phospholipid structure. *Chem Phys Lipids* 1986;39:185–191.
46. Hoekstra D, De Boer T, Klappe K, Wilschut J. Fluorescence method for measuring the kinetics of fusion between biological membranes. *Biochemistry* 1984;23:5675–5681.
47. Ellens H, Bentz J, Szoka FC. H⁺ and Ca²⁺-induced fusion and destabilization of liposomes. *Biochemistry* 1985;24:3099–3106.
48. Sreerama N, Woody RW. Estimation of protein secondary structure from CD spectra: comparison of CONTIN, SELCON and CDSSTR methods with an expanded reference set. *Anal Biochem* 2000;287:252–260.
49. Eisenberg D, Weiss R, Terwilliger T. The helical hydrophobic moment: a measure of the amphiphilicity of the α -helix. *Nature* 1982;299:371–374.
50. Jonson PH, Petersen SB. A critical view on conservative mutations. *Protein Eng* 2001;14:397–402.
51. Hofmann MW, Weise K, Ollesch J, Agrawal P, Stalz H, Stelzer W, Hulsbergen F, de Groot H, Gerwert K, Reed J, Langosch D. De novo design of conformationally flexible transmembrane peptides

- driving membrane fusion. *Proc Natl Acad Sci USA* 2004;101:14776–14781.
52. Brasseur R, Lorge P, Espion D, Goormaghtigh E, Burny A, Ruyschaert JM. The Mode of insertion of the paramyxovirus F1 N-terminus into lipid matrix, an initial step in host cell-virus fusion. *Virus Genes* 1988;1:325–332.
 53. Vonèche V, Portetelle D, Kettman R, Willems L, Limbach K, Paoletti E, Ruyschaert JM, Burny A, Brasseur R. Fusogenic segment of bovine leucemia virus and simian immunodeficiency virus are interchangeable and mediate fusion by means of oblique insertion in the lipid bilayer of their target cells. *Proc Natl Acad Sci USA* 1992;89:3810–3814.
 54. Du HN, Tang L, Luo XY, Li HT, Hu J, Zhou JW, Hu HY. A peptide motif consisting of glycine, alanine, and valine is required for the fibrillization and cytotoxicity of human α -synuclein. *Biochemistry* 2003;42:8870–8878.
 55. Brasseur R, Ruyschaert JM. Conformation and mode of organization of amphiphilic membrane components: a conformational analysis. *Biochem J* 1986;238:1–11.
 56. Lins L, El Kirat K, Flore C, Stroobant V, Thomas A, Brasseur R. Lipid-destabilizing properties of the hydrophobic helices H8 and H9 from colicin E1. *Mol Membr Biol*, in press.
 57. Conway KA, Lee SJ, Rochet JC, Ding TT, Williamson RE, Lansbury PT. Acceleration of oligomerization, not fibrillization, is a shared property of both α -synuclein mutations linked to early-onset Parkinson's disease: implications for pathogenesis and therapy. *Proc Natl Acad Sci USA* 2000;97:571–576.
 58. Goldberg MS, Lansbury PT, Jr. Is there a cause-and-effect relationship between α -synuclein fibrillization and Parkinson's disease? *Nat Cell Biol* 2000;2:115–119.
 59. Lashuel HA, Hartley D, Petre BM, Walz T, Lansbury PT. Neurodegenerative disease: amyloid pores from pathogenic mutations. *Nature* 2002;418:291–291.
 60. Volles MJ, Lansbury PT. Vesicle permeabilization by protofibrillar α -synuclein is sensitive to Parkinson's disease-linked mutations and occurs by a pore-like mechanism. *Biochemistry* 2002;41:4595–4602.
 61. Pountney DL, Lowe R, Quilty M, Vickers JC, Voelcker NH, Gai WP. Annular α -synuclein species from purified multiple system atrophy inclusions. *J Neurochem* 2004;90:502–512.
 62. Lins L, Charlotiaux B, Thomas A, Brasseur R. Implication of a structural motif in the instability of a toxic protein: the Prion. In: Renaville R, Burny A, editors. *Biotechnology in animal husbandry*. Boston, MA: Kluwer; 2001. pp 15–32.
 63. Quist A, Doudevski I, Lin H, Azimova R, Ng D, Frangione B, Kagan B, Ghiso J, Lal R. Amyloid ion channels: a common structural link for protein-misfolding disease. *Proc Natl Acad Sci USA* 2005;102:10427–10432.
 64. Lin H, Bhatia R, Lal R. Amyloid β protein forms ion channels: implications for Alzheimer's disease pathophysiology. *FASEB J* 2001;15:2433–2444.
 65. Apetri MM, Maiti NC, Zagorski MG, Carey PR, Anderson VE. Secondary structure of α -synuclein oligomers: characterization by raman and atomic force microscopy. *J Mol Biol* 2006;355:63–71.
 66. Kirkitadze MD, Condron MM, Teplow DB. Identification and characterization of key kinetic intermediates in amyloid β -protein fibrillogenesis. *J Mol Biol* 2001;312:1103–1119.
 67. Crowther RA, Jakes R, Spillantini MG, Goedert M. Synthetic filaments assembled from C-terminally truncated α -synuclein. *FEBS Lett* 1998;436:309–312.
 68. Lins L, Thomas-Soumarmon A, Pillot T, Vandekerckhove J, Rosseneu M, Brasseur R. Molecular determinants of the interaction between the C-terminal domain of Alzheimer's β -amyloid peptide and apolipoprotein E α -helices. *J Neurochem* 1999;73:758–769.
 69. Pillot T, Goethals M, Najib J, Labeur C, Lins L, Chambaz J, Brasseur R, Vandekerckhove J, Rosseneu M. β -amyloid peptide interacts specifically with the carboxy-terminal domain of human apolipoprotein E: relevance to Alzheimer's disease. *J Neurochem* 1999;72:230–237.
 70. Decaffmeyer M, Lins L, Charlotiaux B, VanEyck MH, Thomas A, Brasseur R. Rational design of complementary peptides to the β Amyloid 29-42 fusion peptide: an application of PepDesign. *Biochim Biophys Acta* 2006;1758:320–327.